

RNA-Based Fluorescent Biosensors for Live Cell Imaging of Second Messenger Cyclic di-AMP

Colleen A. Kellenberger,^{||,†} Chen Chen,^{||,‡} Aaron T. Whiteley,[§] Daniel A. Portnoy,^{‡,§} and Ming C. Hammond^{*,†,‡}

[†]Department of Chemistry, University of California, Berkeley, California 94720, United States

[‡]Department of Molecular & Cell Biology, University of California, Berkeley, California 94720, United States

[§]School of Public Health, University of California, Berkeley, California 94720, United States

Supporting Information

ABSTRACT: Cyclic di-AMP (cdiA) is a second messenger predicted to be widespread in Gram-positive bacteria, some Gram-negative bacteria, and Archaea. In the human pathogen *Listeria monocytogenes*, cdiA is an essential molecule that regulates metabolic function and cell wall homeostasis, and decreased levels of cdiA result in increased antibiotic susceptibility. We have generated fluorescent biosensors for cdiA through fusion of the Spinach2 aptamer to ligand-binding domains of cdiA riboswitches. The biosensor was used to visualize intracellular cdiA levels in live *L. monocytogenes* strains and to determine the catalytic domain of the phosphodiesterase PdeA. Furthermore, a flow cytometry assay based on this biosensor was used to screen for diadenylate cyclase activity and confirmed the enzymatic activity of DisA-like proteins from *Clostridium difficile* and *Methanocaldococcus jannaschii*. Thus, we have expanded the development of RNA-based biosensors for *in vivo* metabolite imaging in Gram-positive bacteria and have validated the first dinucleotide cyclase from Archaea.

Cyclic dinucleotides are an expanding class of second messengers with key roles in bacterial and eukaryotic signaling.¹ A recent addition to this class, cyclic di-AMP (cdiA), regulates processes including bacterial sporulation, ion transport, cell wall homeostasis, and central metabolism in many Gram-positive and pathogenic bacteria, and is the only cyclic dinucleotide predicted in Archaea.^{2,3} In the bacterial pathogens *Staphylococcus aureus* and *Listeria monocytogenes*, decreased levels of cdiA result in increased susceptibility to peptidoglycan-targeting antibiotics,^{4,5} which makes this pathway interesting from a drug targeting perspective. Additionally, secretion of cdiA by *L. monocytogenes* into the cytosol of infected murine macrophage cells elicits a type I interferon response,⁶ and further studies have shown the efficacy of cyclic dinucleotides as small molecule adjuvants.⁷ However, many aspects of cdiA signaling still need to be elucidated, including its homeostasis, metabolic regulatory activity, secretory mechanism, and its function in other microorganisms.

To target this pathway or to further elucidate the role of cdiA in pathogenesis, a robust method for *in vivo* detection of cdiA is required. Direct methods for detection of cdiA include HPLC-

MS, dye intercalation assays, and a competitive ELISA assay,^{8–10} each of which are limited to *in vitro* detection. A cell line harboring an IFN β -luciferase reporter has been used to indirectly detect secreted cdiA.^{5,6} However, to our knowledge, no sensor for live cell imaging of cdiA has yet been reported.

Recently, we and others have generated novel fluorescent biosensors by combining the ligand-sensing domain of different riboswitches or *in vitro* selected aptamers with the profluorescent dye-binding aptamer Spinach (Figure 1a).^{11,12} Here we report the development of two RNA-based biosensors for cdiA that exhibit ligand-induced fluorescence activation *in vitro* and *in vivo*. These fluorescent biosensors were used to examine the levels of cdiA in live *L. monocytogenes* strains by fluorescence microscopy and flow cytometry. To our knowledge, we have generated the first *in vivo* biosensor for cdiA and demonstrated the first application of RNA-based biosensors in a Gram-positive bacterium. Finally, we have applied the biosensor to detect the activity of putative diadenylate cyclases from *Clostridium difficile*, a nosocomial human pathogen, and from *Methanocaldococcus jannaschii*, a thermophilic methanogenic archaea. The latter result provides the first experimental evidence that cyclic dinucleotide signaling extends to Archaea, in addition to bacteria and eukaryotes.^{1,13}

The ydaO riboswitch class recently was identified to bind cdiA with high affinity and selectivity.¹⁴ Structural probing experiments did not pinpoint the ligand binding site, although it was shown that the pseudoknot outside of the first pairing stem (P1) was not required for ligand binding.¹⁴ Thus, several truncations of the riboswitch aptamer from the ydaO gene in *Bacillus subtilis* were fused to the Spinach2 aptamer¹⁵ and tested for cdiA-dependent fluorescence activation (Figures 1b and S1). However, none demonstrated fluorescence activation. In contrast, two constructs in which the related riboswitch aptamer from the yuaA gene in *B. subtilis* was fused to Spinach2 showed some fluorescence activation (2.4-fold for P1–6 and 9.1-fold for P1–4). Screening P1–4 variants of other phylogenetic representatives of this riboswitch class did not identify any with improved fluorescence activation (Figure S2). We instead observed several that exhibit consistent fluorescence deactivation, similar to ydaO P1–4 and P1–5. While turn-off biosensors may be useful to pursue in the future, we initially

Received: January 9, 2015

Published: May 12, 2015

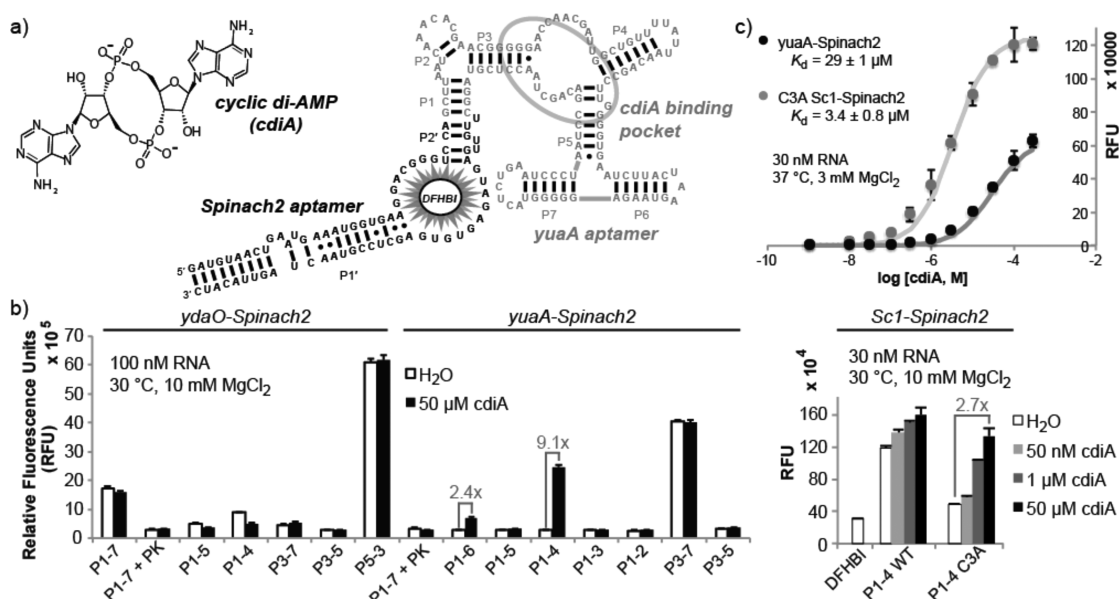


Figure 1. Development of cyclic di-AMP biosensors based on riboswitch-Spinach2 aptamer fusions. (a) Sequence and secondary structure model of yuaA-Spinach2 P1–4 construct. The yuaA riboswitch aptamer (gray) binds cyclic di-AMP and the Spinach2 aptamer (black) binds the profluorescent dye DFHBI. (b) Fluorescence activation screen for the site of Spinach2 attachment to different riboswitch aptamers. Labels indicate the riboswitch stem number followed by the number of base pairs included in the stem. Error bars represent standard deviation between two (Sc1) or three (ydaO, yuaA) independent replicates. (c) *In vitro* binding affinity measurements for two biosensors for cyclic di-AMP. The average from three independent replicates and the best-fit curve are shown. Hill coefficients were 0.94 ± 0.05 for yuaA-Spinach2 and 0.97 ± 0.03 for C3A Sc1-Spinach2. Background fluorescence (without ligand) was subtracted from all data points.

focused on two candidate biosensors with P1–4 stems, yuaA-Spinach2 and Sc1-Spinach2, because they demonstrated high fold turn-on and ligand sensitivity, respectively.

In contrast to yuaA-Spinach2, the Sc1-Spinach2 biosensor not only displays some fluorescence activation with 50 nM cdiA but also exhibits much higher background. Several types of destabilizing mutations to the P1–4 stem of Sc1-Spinach2 were made in order to reduce fluorescence background (Figure S3). Replacement of a C–G base pair with an A–G mismatch via the C3A mutation led to a biosensor with 2.7-fold fluorescence activation and stronger binding affinity relative to yuaA-Spinach2 (Figure 1c). Both biosensors responded selectively to cdiA versus other cyclic dinucleotides and adenosine containing compounds at ligand concentrations up to 100 μM (Figure S4). The lower dissociation constant for C3A Sc1-Spinach2 appears to be due primarily to faster association kinetics (Figure S5).

The X-ray crystal structures of ydaO class riboswitch aptamers recently revealed that two molecules of cdiA are bound in an RNA fold that exhibits pseudo 2-fold symmetry.^{16–18} This finding was unexpected, and in retrospect, attachment to the P1–4 stem removes the 3' peripheral end of the pseudoknot that forms part of one cdiA binding site. Fortunately, mutation of this binding site reduced ligand affinity only 5-fold,¹⁶ and our results also corroborate that this binding site is nonessential. However, the importance of this region to the global RNA fold may explain why biosensor constructs are so sensitive to minor changes in P1 stem length, and why most phylogenetic variants are nonfunctional.

To our advantage, both biosensors harbor a single ligand binding site and display 1:1 stoichiometry of binding to cdiA that gives a good dynamic range of detection (Figure 1c). The *in vitro* fluorescence signal changed from 10% to 90% between 3.2 and 260 μM cdiA for yuaA-Spinach2 and between 0.37 and

30 μM for Sc1-Spinach2. Together, these biosensors can detect cdiA concentrations spanning 4 orders of magnitude. However, it should be noted that the fold change in fluorescence is more modest and not directly proportional to the fold change in ligand concentration.

For intracellular detection of cdiA, yuaA-Spinach2 was preferred due to its low background fluorescence. While no *in vivo* measurements of cdiA levels have previously been made, HPLC analysis of cell extracts of *Bacillus subtilis* and *S. aureus* cultures indicates low micromolar concentrations of cdiA in cells.^{4,8} Thus, this biosensor should be able to detect cdiA at physiologically relevant concentrations.

We were interested in testing the utility of cdiA biosensors in *L. monocytogenes*, a Gram-positive bacterium and human pathogen that has served as an important model for cdiA signaling. Fluorescence microscopy confirmed that DFHBI was able to permeate through the thicker peptidoglycan layer, and expression of Spinach2 in a tRNA scaffold in turn leads to observable cellular fluorescence in *L. monocytogenes* (Figure S6). This result also demonstrates that a strong, constitutive promoter provides sufficient expression of Spinach2-based constructs for visualization in bacteria, avoiding the need to engineer an induction system (Figure S7).

To test the ability of the yuaA-Spinach2 fluorescent biosensor to detect cdiA in live cells, plasmid encoding the biosensor in a tRNA scaffold was transformed into strains of *L. monocytogenes*. For quantitation by flow cytometry, the recently described DFHBI-1T dye¹⁹ dramatically improved the resolution (Figure S8). In comparison to wild type, a $\Delta pdeA$ mutant carrying a deletion of the *pdeA* gene that encodes a cdiA phosphodiesterase⁵ exhibited increased cellular fluorescence (Figure 2a,b). Conversely, decreased cellular fluorescence is observed for the $\Delta dacA \Delta relAPQ$ deletion strain, which rescues the lethality of knocking out *dacA*, the only diadenylate cyclase

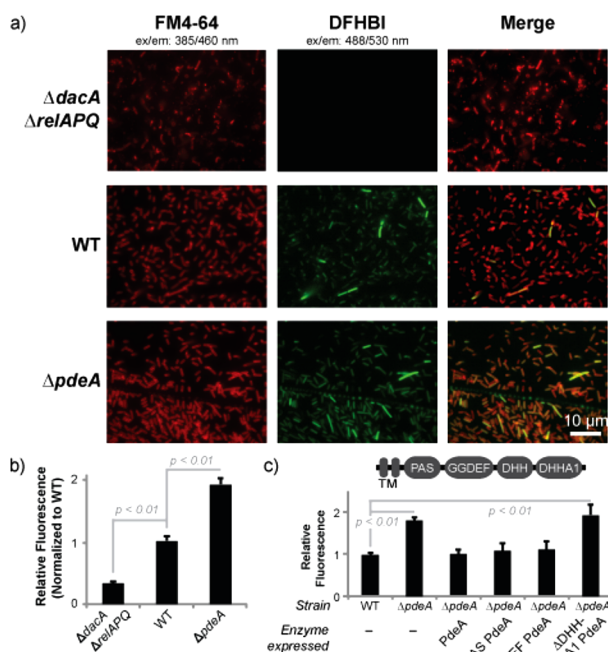


Figure 2. YuaA-Spinach2 biosensor detects altered cyclic di-AMP levels in *Listeria monocytogenes*. (a) Fluorescence microscopy images of *L. monocytogenes* 10403s strains expressing yuaA-Spinach2 tRNAs after incubation with the membrane dye FM4-64 or DFHBI (left and middle panels, respectively; right panels show merge). (b) Flow cytometry analysis of *L. monocytogenes* strains expressing yuaA-Spinach2 tRNAs. Error bars represent standard deviation between four independent biological replicates. (c) Flow cytometry analysis of WT or $\Delta pdeA$ strains with no complementation or complemented with different PdeA enzyme constructs. The domain arrangement for PdeA is shown; the transmembrane (TM) domain was not included in the enzyme constructs. Error bars represent standard deviation between three independent biological replicates.

gene.²⁰ In contrast, expression and fluorescent visualization of Spinach2 showed no significant change in these strains (Figure S6). Thus, the data are consistent with the yuaA-Spinach2 biosensor giving a fluorescent read-out of differences in endogenous cdiA concentrations for mutant versus wild-type strains of *Listeria*.

Furthermore, we showed that the yuaA-Spinach2 biosensor could be employed in a complementation assay in *Listeria*. The *in vivo* catalytic activity of the pdeA gene constructs harboring different domain deletions was assessed by coexpression with the biosensor in the $\Delta pdeA$ mutant background. Whereas the full-length enzyme or truncated versions lacking either the PAS or GGDEF domains rescued phosphodiesterase activity, constructs without the C-terminal DHH and DHHA1 domains showed no rescue of activity (Figure 2c). This result is consistent with the DHH domain being the catalytic domain of the phosphodiesterase, as shown for GdpP phosphodiesterase, a homologue in *B. subtilis*.²¹

Finally, we applied the biosensor toward assaying the *in vivo* catalytic activity of putative diadenylate cyclases (DACs) by heterologous expression in *E. coli* (Figure 3a). Coexpression of biosensors specific for each bacterial cyclic dinucleotide^{11,22} with each of three confirmed dinucleotide cyclases demonstrated that each biosensor distinguishes production of specific cyclic dinucleotides (Figure 3b, Table S1). For instance, the yuaA-Spinach2 biosensor exhibited a ~ 12 -fold fluorescence

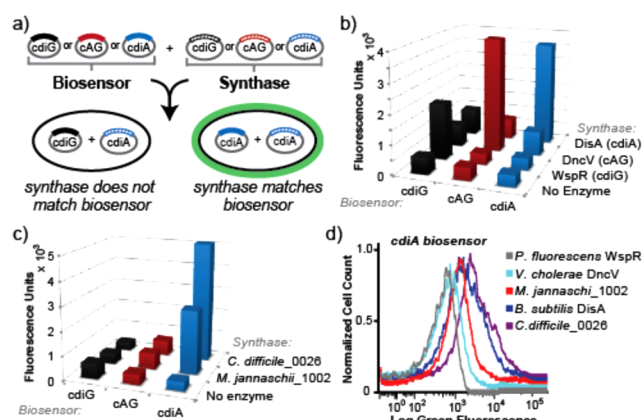


Figure 3. An *in vivo* activity assay for novel diadenylate cyclases using cyclic dinucleotide-selective biosensors. (a) Schematic of the two plasmid screening system. *E. coli* is cotransformed with a biosensor-encoding plasmid and an enzyme-encoding plasmid. After induction of expression, cells are incubated with DFHBI-1T and fluorescence is analyzed. (b) Flow cytometry data for biosensors upon coexpression with no enzyme or a known diguanylate cyclase (WspR), cyclic AMP-GMP synthase (DncV), or diadenylate cyclase (DisA). (c) Flow cytometry data for biosensors upon coexpression with predicted diadenylate cyclases from *M. jannaschii* and *C. difficile*. Fluorescence values from (b) and (c) are the average of three independent replicates and are shown with standard deviations in Table S1. (d) Representative flow cytometry graph for the yuaA-Spinach2 biosensor using logicle scaling on x-axis.

activation in response to coexpression of a known DAC, DisA from *Bacillus subtilis*, relative to no enzyme. In contrast, coexpression with WspR led to little change and coexpression with DncV led to a modest change (~ 2 -fold) in fluorescence that may be due to promiscuous enzyme activity²³ or slight cross-sensitivity of the biosensor.

While more than 2000 DAC domains have been predicted across bacteria and select archaea,²⁴ only a handful of enzymes have been confirmed in bacteria. Furthermore, cyclic dinucleotide signaling has yet to be demonstrated in Archaea. Thus, we analyzed single DAC genes predicted in the genomes of *Clostridium difficile* (gene id: 0026), a ubiquitous human pathogen, and *Methanocaldococcus jannaschii* (gene id: 1002), an important methane-producing archaea. Coexpression of either putative DAC genes with the cdiG- or cAG-specific biosensor produced no significant fluorescence above background. With the cdiA biosensor, however, ~ 13 - and ~ 7 -fold fluorescence activation over background was observed in response to the *C. difficile* and *M. jannaschii* enzymes, respectively (Figure 3c,d). These results demonstrate that these enzymes are active DACs, which was confirmed through cell extract analysis (Figure S9), and thus expand cyclic dinucleotide signaling to all three domains of life.

In summary, we have developed RNA-based biosensors for cdiA that enable live cell imaging of this second messenger in *Listeria* and *E. coli*. The application of these biosensors has been demonstrated for screening bacterial strains, mapping enzymatic domains, and testing candidate enzymes from heterologous organisms. Most notably, we validated the activity of an archaeal DAC and the only predicted DAC in *C. difficile*. However, to monitor subtle fluctuations in cdiA levels that may occur in response to cellular and environmental conditions, the sensitivity and fluorescence turn-on properties of these biosensors would need to be improved. Also, robust methods

to normalize the fluorescence signal under different conditions will need to be developed.

It is interesting that despite the structural similarity of the three bacterial cyclic dinucleotides, distinct enzyme classes have been found to produce each one. Whether any organisms have evolved other mechanisms to synthesize cyclic dinucleotides remains an open question. We envision that the selective biosensors reported here will enable validation of other predicted dinucleotide cyclases and will potentiate the discovery of previously unidentified signaling domains.

■ ASSOCIATED CONTENT

📄 Supporting Information

Methods and supplementary data. The Supporting Information is available free of charge on the ACS Publications website at DOI: 10.1021/jacs.5b00275.

■ AUTHOR INFORMATION

Corresponding Author

*mingch@berkeley.edu

Author Contributions

[†]C.A.K. and C.C. contributed equally.

Notes

The authors declare the following competing financial interest(s): Daniel A. Portnoy has a consulting relationship with and a financial interest in Aduro BioTech, and both he and the company stand to benefit from the commercialization of the results of this research.

■ ACKNOWLEDGMENTS

We thank Zachary Hallberg for assistance in cell extraction assays. This work is supported in part by NIH 1DP2 OD008677 (M.C.H.), NIH 1P01 AI63302 (D.A.P.), 1R01 AI27655 (D.A.P.), DoD NDSEG fellowship (C.A.K.), and NSF graduate fellowship DGE 1106400 (A.T.W.). M.C.H. holds a Career Award at the Scientific Interface from the Burroughs Wellcome Fund.

■ REFERENCES

- (1) Danilchanka, O.; Mekalanos, J. J. *Cell* **2013**, *154*, 962.
- (2) Corrigan, R. M.; Gründling, A. *Nat. Rev. Microbiol.* **2013**, *11*, 513.
- (3) Sureka, K.; Choi, P. H.; Precit, M.; Delince, M.; Pensinger, D. A.; Huynh, T. N.; Jurado, A. R.; Goo, Y. A.; Sadilek, M.; Iavarone, A. T.; Sauer, J.-D.; Tong, L.; Woodward, J. J. *Cell* **2014**, *158*, 1389.
- (4) Corrigan, R. M.; Abbott, J. C.; Burhenne, H.; Kaever, V.; Gründling, A. *PLoS Pathog.* **2011**, *7*, e1002217.
- (5) Witte, C. E.; Whiteley, A. T.; Burke, T. P.; Sauer, J.-D.; Portnoy, D. A.; Woodward, J. J. *MBio* **2013**, *4*.
- (6) Woodward, J. J.; Iavarone, A. T.; Portnoy, D. A. *Science* **2010**, *328*, 1703.
- (7) Libanova, R.; Becker, P. D.; Guzmán, C. A. *Microb. Biotechnol.* **2012**, *5*, 168.
- (8) Oppenheimer-Shaanan, Y.; Wexselblatt, E.; Katzhendler, J.; Yavin, E.; Ben-Yehuda, S. *EMBO Rep.* **2011**, *12*, 594.
- (9) Bai, Y.; Yang, J.; Eisele, L. E.; Underwood, A. J.; Koestler, B. J.; Waters, C. M.; Metzger, D. W.; Bai, G. J. *Bacteriol.* **2013**, *195*, 5123.
- (10) Zhou, J.; Sayre, D. A.; Zheng, Y.; Szmecinski, H.; Sintim, H. O. *Anal. Chem.* **2014**, *86*, 2412.
- (11) Kellenberger, C. A.; Wilson, S. C.; Sales-Lee, J.; Hammond, M. C. *J. Am. Chem. Soc.* **2013**, *135*, 4906.
- (12) Paige, J. S.; Nguyen-Duc, T.; Song, W.; Jaffrey, S. R. *Science* **2012**, *335*, 1194.
- (13) Schaap, P. *IUBMB Life* **2013**, *65*, 897.

- (14) Nelson, J. W.; Sudarsan, N.; Furukawa, K.; Weinberg, Z.; Wang, J. X.; Breaker, R. R. *Nat. Chem. Biol.* **2013**, *9*, 834.
- (15) Strack, R. L.; Disney, M. D.; Jaffrey, S. R. *Nat. Methods* **2013**, *10*, 1219.
- (16) Gao, A.; Serganov, A. *Nat. Chem. Biol.* **2014**, *10*, 787.
- (17) Ren, A.; Patel, D. J. *Nat. Chem. Biol.* **2014**, *10*, 780.
- (18) Jones, C. P.; Ferré-D'Amaré, A. R. *EMBO J.* **2014**, *33*, 2692.
- (19) Song, W.; Strack, R. L.; Svensen, N.; Jaffrey, S. R. *J. Am. Chem. Soc.* **2014**, *136*, 1198.
- (20) Whiteley, A. T.; Pollock, A. J.; Portnoy, D. A. *Cell Host & Microbe* **2015**, DOI: 10.1016/j.chom.2015.05.006.
- (21) Rao, F.; See, R. Y.; Zhang, D.; Toh, D. C.; Ji, Q.; Liang, Z.-X. *J. Biol. Chem.* **2010**, *285*, 473.
- (22) Kellenberger, C. A.; Wilson, S. C.; Hickey, S. F.; Gonzalez, T. L.; Hallberg, Z. F.; Brewer, T. F.; Iavarone, A. T.; Carlson, H. K.; Hsieh, Y.-F.; Hammond, M. C. *Proc. Natl. Acad. Sci. U.S.A.* **2015**, *112*, 5383.
- (23) Davies, B. W.; Bogard, R. W.; Young, T. S.; Mekalanos, J. J. *Cell* **2012**, *149*, 358.
- (24) Romling, U. *Sci. Signal.* **2008**, *1*, pe39.